

# Ornithine- $\delta$ -Aminotransferase Inhibits Neurogenesis During *Xenopus* Embryonic Development

Ying Peng,<sup>1</sup> Sandra K. Cooper,<sup>2</sup> Yi Li,<sup>1</sup> Jay M. Mei,<sup>3</sup> Shuwei Qiu,<sup>1</sup> Gregory L. Borchert,<sup>2</sup> Steven P. Donald,<sup>3</sup> Hsiang-fu Kung,<sup>4</sup> and James M. Phang<sup>3</sup>

<sup>1</sup>Department of Neurology, Sun Yat-sen Memorial Hospital, Sun Yat-sen University, Guangzhou, China

<sup>2</sup>Basic Research Program, Leidos, Inc., National Cancer Institute at Frederick, National Institutes of Health, Frederick, Maryland, United States

<sup>3</sup>Metabolism and Cancer Susceptibility Section, Basic Research Laboratory, National Cancer Institute at Frederick, National Institutes of Health, Frederick, Maryland, United States

<sup>4</sup>State Key Laboratory of Oncology in Southern China, and Centre for Emerging Infectious Diseases, the Chinese University of Hong Kong, Shatin, Hong Kong, China

Correspondence: Ying Peng, Department of Neurology, Sun Yat-sen Memorial Hospital, Sun Yat-sen University, Guangzhou, China; 2353352460@qq.com.

James M. Phang, Metabolism and Cancer Susceptibility Section, Basic Research Laboratory, National Cancer Institute at Frederick, National Institutes of Health, Frederick, MD, USA;

phangj@mail.nih.gov.

Submitted: January 21, 2015

Accepted: March 8, 2015

Citation: Peng Y, Cooper SK, Li Y, et al. Ornithine- $\delta$ -aminotransferase inhibits neurogenesis during *Xenopus* embryonic development. *Invest Ophthalmol Vis Sci*. 2015;56:2486–2497. DOI:10.1167/iovs.15-16509

**PURPOSE.** In humans, deficiency of ornithine- $\delta$ -aminotransferase (OAT) results in progressive degeneration of the neural retina (gyrate atrophy) with blindness in the fourth decade. In this study, we used the *Xenopus* embryonic developmental model to study functions of the OAT gene on embryonic development.

**METHODS.** We cloned and sequenced full-length OAT cDNA from *Xenopus* oocytes (X-OAT) and determined X-OAT expression in various developmental stages of *Xenopus* embryos and in a variety of adult tissues. The phenotype, gene expression of neural developmental markers, and enzymatic activity were detected by gain-of-function and loss-of-function manipulations.

**RESULTS.** We showed that X-OAT is essential for *Xenopus* embryonic development, and overexpression of X-OAT produces a ventralized phenotype characterized by a small head, lack of axial structure, and defective expression of neural developmental markers. Using X-OAT mutants based on mutations identified in humans, we found that substitution of both Arg 180 and Leu 402 abrogated both X-OAT enzymatic activity and ability to modulate the developmental phenotype. Neurogenesis is inhibited by X-OAT during *Xenopus* embryonic development.

**CONCLUSIONS.** Neurogenesis is inhibited by X-OAT during *Xenopus* embryonic development, but it is essential for *Xenopus* embryonic development. The Arg 180 and Leu 402 are crucial for these effects of the OAT molecule in development.

**Keywords:** *Xenopus*, embryos, development, neuralization, ventralization

Pyrroline-5-carboxylate (P5C), the precursor and immediate degradative product of proline, participates in a redox shuttle in which the cycling of proline and P5C transfers reducing (oxidizing) potential into and out of mitochondria.<sup>1,2</sup> In the brain, proline enters neurons via a high-affinity transporter<sup>3,4</sup> and proline acts as a neurotransmitter by inhibiting glutamatergic neurons. Mutations in proline dehydrogenase coding for proline oxidase results in neurologic defects in animals<sup>5</sup> and is associated with susceptibility to schizophrenia.<sup>6,7</sup> Studies into the mechanism of this association can take advantage of two other pathways that generate P5C. Pyrroline-5-carboxylate synthase generates P5C from glutamate,<sup>8</sup> and mutations in the gene encoding this enzyme have been associated with neurodegeneration, cataracts, and connective tissue disease,<sup>9,10</sup> but mechanistic studies in this disorder have only begun. On the other hand, ornithine- $\delta$ -aminotransferase (OAT), which produces P5C from ornithine,<sup>8</sup> has been intensively studied, and defects in OAT result in a well-characterized clinical disorder with a defect in neural tissue.<sup>11</sup>

Ornithine- $\delta$ -aminotransferase is a pyridoxal phosphate-dependent mitochondrial matrix enzyme expressed in most

mammalian tissues, including the kidney, liver, small intestine, and retina. Ornithine- $\delta$ -aminotransferase catalyzes the reversible transamination of ornithine to glutamic- $\gamma$ -semialdehyde, an intermediate in proline and glutamate metabolism.<sup>12</sup> In humans, deficiency of OAT is inherited as an autosomal recessive trait and results in gyrate atrophy (GA) of the choroid and retina, a progressive chorioretinal degeneration, with blindness occurring by the fourth decade.<sup>12–14</sup> Simell and Takki<sup>15</sup> reported that hyperornithinemia and overflow ornithine were present in GA patients, and Valle et al.<sup>16</sup> showed that OAT deficiency was the primary cause of GA. Subsequently, the human OAT gene was cloned and mapped (10q26), and more than 60 mutations causing GA have been identified.<sup>14,17–21</sup> Two mouse models with OAT deficiency, one generated by gene targeting<sup>22</sup> and a spontaneous variant,<sup>23</sup> were found to have conditions similar to those in GA patients, including chronic hyperornithinemia, massive orthinuria, and progressive retinal degeneration. Studies of the OAT-deficient mouse also revealed that an arginine-restricted diet substantially reduced plasma ornithine levels and completely prevented retinal degeneration.<sup>24</sup> Treatment for GA is still a daunting task,

in part because of our limited understanding of the pathogenesis of chorioretinal degeneration. Central to this challenge is the more complete understanding of the functions of the OAT gene and the function of the gene product in epigenetic regulation.

*Xenopus laevis* has been widely used for functional genomics studies,<sup>25,26</sup> and it is widely used to study gene function by manipulating expression with transiently expressed RNA or DNA injected into fertilized eggs or early cleavage embryos. In early development, zygotic gene activation occurs at the midblastula transition after initial cell division driven by maternal factors.<sup>27</sup> Subsequently, signaling centers, such as the Nieuwkoop Center and the Organizer, impart a dorsal character to the mesoderm and the overlying ectoderm after zygotic activation. Transcriptional and metabolic modulation of these factors are of particular interest, as elucidation of the components that regulate them is well under way.<sup>28</sup> Fetal development is normal in mice models with OAT deficiency.<sup>22,23</sup> Because maternal OAT and transplacental metabolism may compensate for the deficiencies in utero, potential effects of OAT in development may be revealed only in lower organisms lacking as-yet-undefined redundant pathways. Other investigators have used *Drosophila melanogaster* and *Caenorhabditis elegans* to reveal developmental aberrations accompanying specific gene mutations.<sup>29,30</sup> Thus, we considered that manipulation of OAT expression during *Xenopus* embryonic development may yield useful insights.

This article describes the functional role of OAT in *Xenopus* embryonic development. A full-length OAT cDNA was cloned and sequenced from *Xenopus* oocytes (X-OAT). We determined X-OAT expression in various developmental stages of *Xenopus* embryos and in a variety of adult tissues. Using in situ hybridization, we found that the X-OAT was expressed predominantly in the brain and spinal cord in the tadpole stage. By gain-of-function and loss-of-function manipulations, we showed that OAT is essential for *Xenopus* embryonic development, and overexpression of X-OAT produces a ventralized phenotype characterized by a small head and short tail, well-patterned ventral tissues, and the lack of apparent axial structures. Using X-OAT mutants, we found that Arg 180 and Leu 402 are crucial for these effects of the OAT molecule in development.

## METHODS

All experimental procedures were approved by the Animal Care and Use Committee of National Cancer Institute-Frederick, National Institutes of Health. The protocol is #99-084 entitled, "Signaling mechanisms in *Xenopus* embryos." All experiments are in compliance with the ARVO policy for the Use of Animals in Ophthalmic and Vision Research.

### Animals

Adult *Xenopus laevis* were bred according to guidelines outlined in the *Xenopus* book.<sup>31</sup> Embryos were incubated at 22°C in MMR medium (0.1 M NaCl, 2.0 mM KCl, 1 mM MgSO<sub>4</sub>, 2 mM CaCl<sub>2</sub>, 5 mM HEPES, pH7.8, 0.1 mM EDTA), and staged according to the external morphology.

### Cloning of the X-OAT and Plasmid Construction

The *Xenopus* homologue of OAT was cloned by RT-PCR. We used 3 µg total RNA isolated from *Xenopus* oocytes and an oligo-dT adapted primer to convert mRNA into cDNA according to the procedure described in the 3' RACE System

for rapid amplification of cDNA ends kit (GibcoBRL, Rockville, MD, USA). The PCR used a gene-specific primer designed from the X-OAT fragment (GenBank, Accession #AW199859) and the abridged universal amplification primer obtained from the kit (primers: forward, 5'-ATGCTTTCCAACTAATCCAGA-3'; reverse, 5'-GGCCACGCGTCGACTAGTAC-3'). The cDNA was ligated into pGEM-T Easy Vector (Promega, Madison, WI, USA) and then sequenced. The full-length clone was amplified using the primers containing a *Pst* I or *Sal* I restriction endonuclease site (forward, 5'-CCTCCTGCAGATGCTTTCCAACTAATCCA-3'; reverse, 5'-TACGGTTCGACTTAGAAAGACAGCAGGGTTT-3'). The full-length PCR product (1.32 kb) was digested with restriction endonucleases (*Pst* I and *Sal* I) and then cloned into pBluescript II SK-plasmid for sequence. The consensus cDNA nucleotide sequences (X-OAT) were found to be highly homologous to those reported in human, mouse, rat, and *Drosophila* genes.<sup>21,32,33</sup>

## Mutagenesis and In Vitro Translation

Mutations were generated using the Quick-Change Site-Directed Mutagenesis Kit (Stratagene, La Jolla, CA, USA), according to the manufacturer's instructions. Based on homologies to human OAT and mutations in GA,<sup>18,34,35</sup> we made the following four mutations: X-OATR180T (M1), X-OATR180T/L402P (M2), X-OATL402P (M3), and X-OATK292N (M4) (Fig. 1). All constructs were sequenced to verify mutations and to ensure that no additional mutations were introduced. The mutants were subcloned into pSP64TEN as previously reported,<sup>36</sup> and capped mRNA was prepared using the MEGA-script in vitro transcription kit (Ambion, Austin, TX, USA). The translation reaction was conducted in a TNT-coupled reticulocyte lysate system (TNT Kit; Promega) in the presence of [35S]methionine (Amersham Pharmacia Biotech, Inc., Piscataway, NJ, USA). The products of the translation reaction were subjected to SDS-PAGE, and dried gels were analyzed by autoradiography.

## Whole-Mount In Situ Hybridization

Embryos were collected from stages 2 to 40 and analyzed for X-OAT expression. In situ hybridization studies were performed using a digoxigenin-labeled (Boehringer-Ingelheim, Ingelheim, Germany) antisense RNA probe or a fluorescein-labeled (Boehringer-Ingelheim) antisense RNA probe. Both probes were synthesized from pBluescript II SK(-)-X-OAT plasmids linearized with *Pst* I by using T7 RNA polymerase. Digoxigenin was detected using alkaline phosphatase-conjugated anti-digoxigenin antibodies (Boehringer-Ingelheim) and 5-bromo,4-chloro,3-indolylphosphate/nitroblue tetrazolium substrates.

## Microinjections and Explant Culture of Embryonic Tissues

The X-OAT construct and mutants of X-OAT were subcloned into pSP64TEN vector for in vitro synthesis of capped sense mRNA using the Sp6 transcription kit (Ambion), according to the manufacturer's instructions. The synthetic RNAs were quantitated by ethidium bromide staining with reference to standard RNA.<sup>25</sup> Embryos of *X. laevis* were obtained by artificial insemination after induction of females with 500 U human chorionic gonadotropin. The developmental stage was designated according to our previous publication.<sup>36</sup> Embryos at the two-cell stage were injected in the animal pole, and at the four-cell stage, they were injected in the dorsal marginal zone with various mRNAs. Animal caps (ACs) were dissected from the injected embryos at stages 8.5 to 9.0 and cultured at 22°C in 67% Leibovitz's L-15 medium (Life

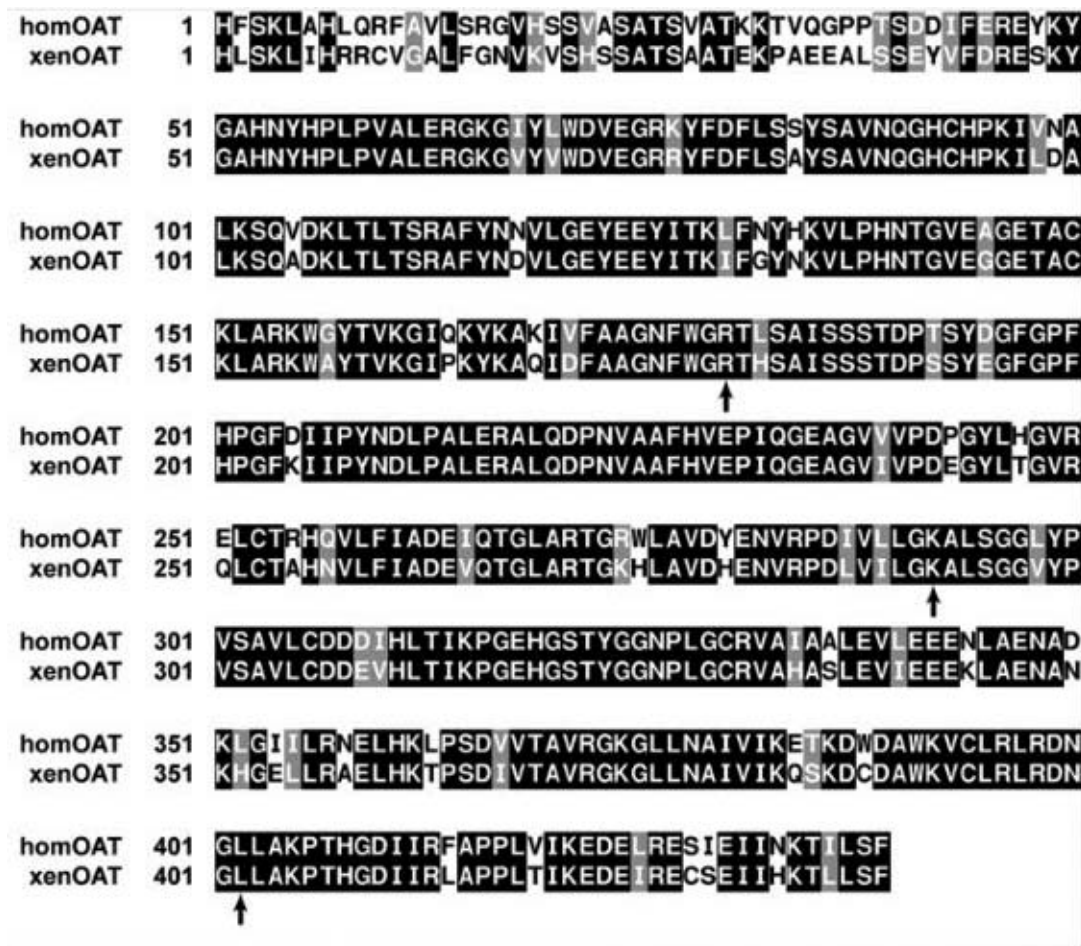


**FIGURE 1.** Comparison of human and *Xenopus* OAT amino acid sequences. Arrows indicate locations of X-OAT mutations generated as described in the Methods section.

Technologies, Inc., Bethesda, MD, USA) with 7 mM Tris-HCl (pH 116. 7.5) and gentamycin (50 µg/mL) to various stages before being harvested for RT-PCR. Noteworthy in these studies was the concentration of L-arginine at 335 mg/L and glutamine at 201 mg/L. There was no added ornithine in this medium.

### Morpholino Antisense Oligonucleotides

The X-OAT morpholino antisense oligonucleotide (X-OAT-Mo), a 25-meroligo, was designed against the 5' untranslated region of *Xenopus* OAT, immediately adjacent to the initiation start site with the following base sequence 5'-TGGATTAGTTTG GAAAGCATTCTGG-3' (Gene Tools, LLC, Philomath, OR, USA). Doses of 5 to 10 ng X-OAT-Mo per embryo were injected into the animal pole area of two-cell stage embryos or ventral marginal zone at the four-cell stage. A sense control morpholino oligonucleotide (Co-Mo) composed of base sequence 5'-CCAGAATGCTTTCCAAACTAATCCA-3' (Gene Tools, LLC) was injected as a control at the same concentration.

### Reverse Transcriptase PCR

Total RNA was extracted from cultured AC explants with TRIzol reagent (Life Technologies, Inc.), following the manufacturer's instructions. Reverse transcriptase PCR was performed using a Superscript Pre-amplification System (Life Technologies, Inc.). Primers were designed as follows: X-

OAT: forward, 5'-CGCGTGGCTATGGCTTCTTT-3', and reverse, 5'-GGAGGAGCCAGCCGGATAAT-3'. Otx2: forward, 5'-GGATG GATTTGTTGCACCAGTC-3' and reverse, 5'-CACTCTCCGA GCTCACTTCTC-3'. Hoxb9: forward, TACTTACGGG CTG GCT G GA, and reverse, 5'-AGCGTGTAACCAGTTGGCTG-3'. Polymerase chain reaction conditions were as follows: 5 minutes at 95°C for 1 cycle; 1 minute at 94°C, 45 seconds at 60°C, and 1 minute at 72°C for 32 cycles. Polymerase chain reaction products were subjected to electrophoresis on Tris acetate EDTA gels and visualized by ethidium bromide staining. Although the data from individual experiments are shown, the results were confirmed in multiple experiments in all cases.

### Ornithine-δ-Aminotransferase Enzyme Activity

Ornithine-δ-aminotransferase activities from the ACs (stage 22) were measured with a radioisotopic assay.<sup>37</sup> The ACs dissected from embryos injected with β-gal, X-OAT (X-OATWT), X-OATR180T, X-OATR180T/L402P, X-OATL402P, X-OATK292N) and X-OAT-Mo mRNAs were sonicated in 100 mM potassium phosphate (pH 8.0). Protein was determined by Lowry assay. The reaction mixture contained 0.5 µCi L-ornithine-C14 (Amersham Pharmacia Biotech, Inc.), 0.7 mM unlabeled ornithine, 0.14 µM pyridoxal phosphate, 0.1 M potassium phosphate (pH 8.0), and 0.7 mM α-ketoglutarate. The AC extracts were incubated with reaction mixture at room temperature (24°C) for 60 minutes, then 50 µL orthoamino-benzaldehyde solution was added to terminate the reaction.

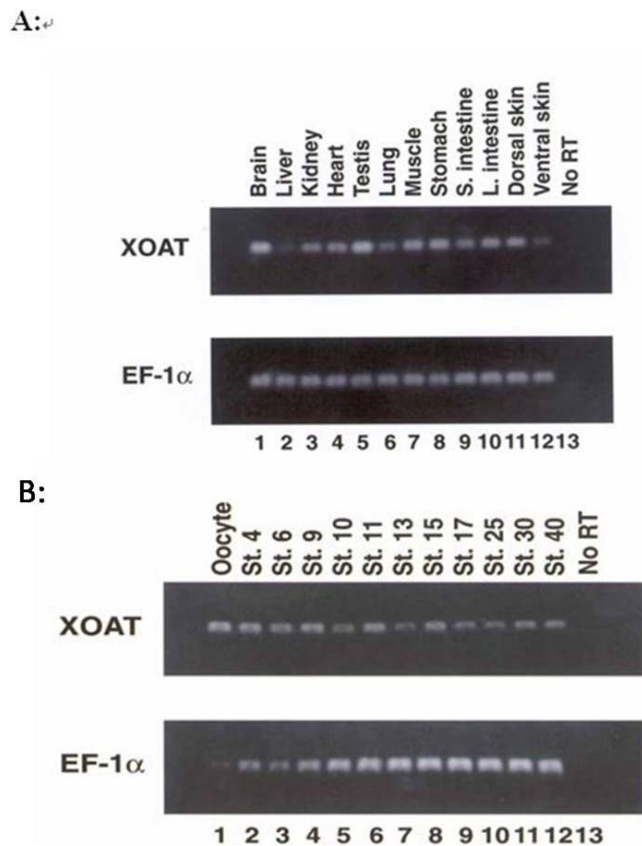


**FIGURE 2.** Expression of *X-OAT* at different developmental stages of *Xenopus* and in different tissues of adult *Xenopus*. Reverse transcriptase PCR analysis of *X-OAT* expression: (A) brain, lane 1; liver, lane 2; kidney, lane 3; heart, lane 4; testis, lane 5; lung, lane 6; muscle, lane 7; stomach, lane 8; small intestine, lane 9; large intestine, lane 10; dorsal skin, lane 11; ventral skin, lane 12. No RTs (lane 13) were performed with total RNAs obtained from the brain tissue and processed through the reactions without RT to confirm the absence of contaminating genomic DNA. Expression of *EF-1α* was tested to serve as a loading control. (B) Oocyte (stages 5–6), lane 1; stage 4, lane 2; stage 6, lane 3; stage 9, lane 4; stage 10, lane 5; stage 11, lane 6; stage 13, lane 7; stage 15, lane 8; stage 17, lane 9; stage 25, lane 10; stage 30, lane 11; stage 40, lane 12. No RT control reactions (lane 13) were performed with total RNAs obtained from the oocyte.

The samples were then centrifuged at 2000g for 5 minutes. The reaction product, glutamate semialdehyde, is converted nonenzymatically to P5C, which is separated from ornithine by ion exchange chromatography on disposable 1-mL Dowex AG 50w-X8 resin form 100- to 200-mesh columns (Sigma-Aldrich Corp., St. Louis, MO, USA).<sup>37</sup> The disintegrations per minute (DPM) for each sample was determined using a multipurpose scintillation counter (LS 6500; Beckman-Coulter, Brea, CA, USA).

## RESULTS

### Nucleotide and Amino Acid Sequences and Phylogenetic Analysis

The OAT isolated from *Xenopus* oocytes in this study was designated *X-OAT* (GenBank AY005479) and has a 1320-bp open reading frame (ORF) encoding an OAT monomer of 439 residues (Fig. 1). Compared with human OAT, *X-OAT* showed 80% identity at the amino acid level. We also compared the sequence of *X-OAT* to that of OAT from mouse, rat, *C. elegans*,

and *Drosophila*. The amino acid alignment of OAT is highly conserved in all species examined (data not shown).

### *X-OAT* Gene Spatio-Temporal Expression During Embryonic Development and Expression Patterns in Various Adult Tissues

The gene expression pattern of *X-OAT* in various adult tissues of a male *Xenopus* was investigated by RT-PCR. We examined the following tissues: brain, liver, kidney, heart, testis, lung, muscle, stomach, small intestine, and large intestine, plus dorsal and ventral skin. Our results show that *X-OAT* is expressed in nearly all tissues and the results are consistent with the findings in mouse, rat, and human expression patterns,<sup>20,32,33</sup> with some minor differences. We found an elevated *X-OAT* expression in the brain and testis of adult *Xenopus* (Fig. 2A). The temporal and spatial patterns of *X-OAT* expression were investigated by RT-PCR and whole-mount in situ hybridization. Reverse transcriptase PCR by semiquantitative analysis revealed that almost the same level of *X-OAT* was expressed from the oocyte to the tadpole stage (stage 40) (Fig. 2B). Whole-mount in situ hybridization revealed that *X-OAT* was ubiquitously expressed in all regions of the oocyte (Fig. 3A). In the early neural development stage, *X-OAT* initially localized in the dorsal side (Fig. 3B), especially in the neural plate. In the tadpole stage, *X-OAT* was predominantly expressed in the brain and spinal cord (Fig. 3C).

### Consequences of Perturbation of *X-OAT* Expression in Early Development

To understand the role of *X-OAT* during embryonic development, we inhibited *X-OAT* expression by microinjecting 5 or 10 ng *X-OAT-Mo* into the animal pole of the two-cell stage embryos individually, then culturing the embryos in 30% MMR. The gastrulation defects were observed with 5 ng *X-OAT-Mo*-injected embryos at late gastrulation stage (stage 13). The 10 ng *X-OAT-Mo*-injected embryos died at early gastrulation stage (stage 10) (Figs. 4A–C). To assess the embryonic activity of *X-OAT* hyperexpression, we injected synthetic sense RNA encoding *X-OAT* into the animal pole of two-cell stage embryos (Fig. 5A) or into the dorsal marginal zone of four-cell stage embryos (Fig. 5B). Injection into either site elicited a similar phenotype of ventralizing malformations, with small heads, well-patterned ventral side, and short tails with the absence of apparent axial structures (56%,  $n = 50$ , injected into animal pole; 68%,  $n = 50$ , injected into dorsal marginal zone) (Figs. 5A, 5B).

### Overexpression of *X-OAT* Inhibits Neurogenesis

The morphological changes induced by *X-OAT* led us to consider whether exogenous *X-OAT* affected neural development. After *X-OAT* mRNA (1 ng) was injected into the animal pole of the two-cell stage embryos, ACs were dissected at stages 8.5 to 9.0 and cultured in 67% Leibovitz's L-15 medium containing activin (10 ng/mL) and retinoic acid ( $10^{-5}$  M) until they reached the equivalent of stage 22. Activin, a member of the TGF- $\beta$  superfamily, can induce differentiation of almost all mesodermal tissue.<sup>38</sup> Retinoic acid, a derivative of vitamin A, is a potent teratogen and affects the differentiation of many cells in vitro. In vertebrates, retinoic acid is apparently involved in the development of the central nervous system.<sup>39</sup> Therefore, both activin A and retinoic acid are good candidates for neural- and mesoderm-inducing factors.<sup>40–42</sup> As shown in Figure 6, ACs dissected from embryos injected

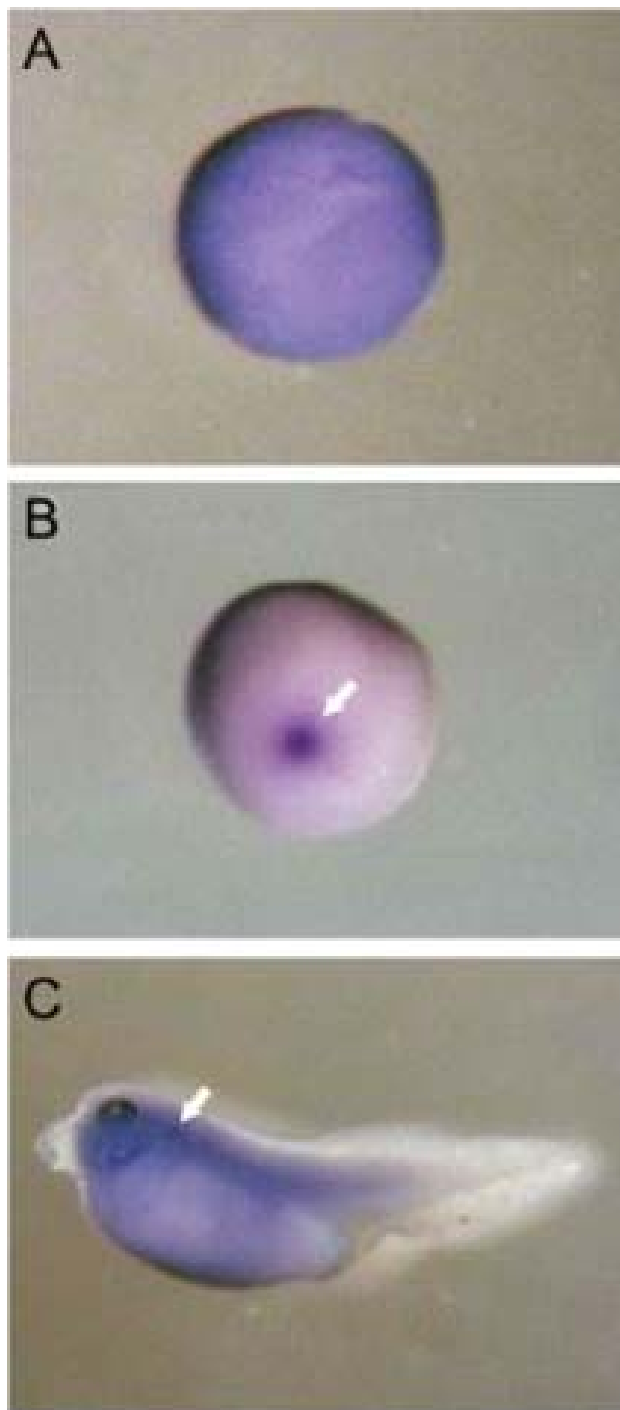


**FIGURE 3.** Spatio-temporal expression of OAT during embryonic development. Whole-mount in situ hybridization analysis shows that (A) *X-OAT* is expressed in all regions of oocyte. (B) In the early neural stage, *X-OAT* is localized principally to the dorsal side, especially in the notoplate (*white arrow*). (C) The *X-OAT* is predominantly expressed in brain and spinal cord at tailbud stage, as shown with digoxigenin-labeling (*white arrow*).

with *X-OAT-Mo* or control  $\beta$ -gal developed a neural-like phenotype: slightly swollen with one side white and the other black (Figs. 6A, 6C). In contrast, *X-OAT* sense-injected ACs developed an epidermal-like phenotype, mostly round and evenly brownish (Fig. 6B). To advance our understanding of the role of the *X-OAT* gene in neurogenesis, an analysis of

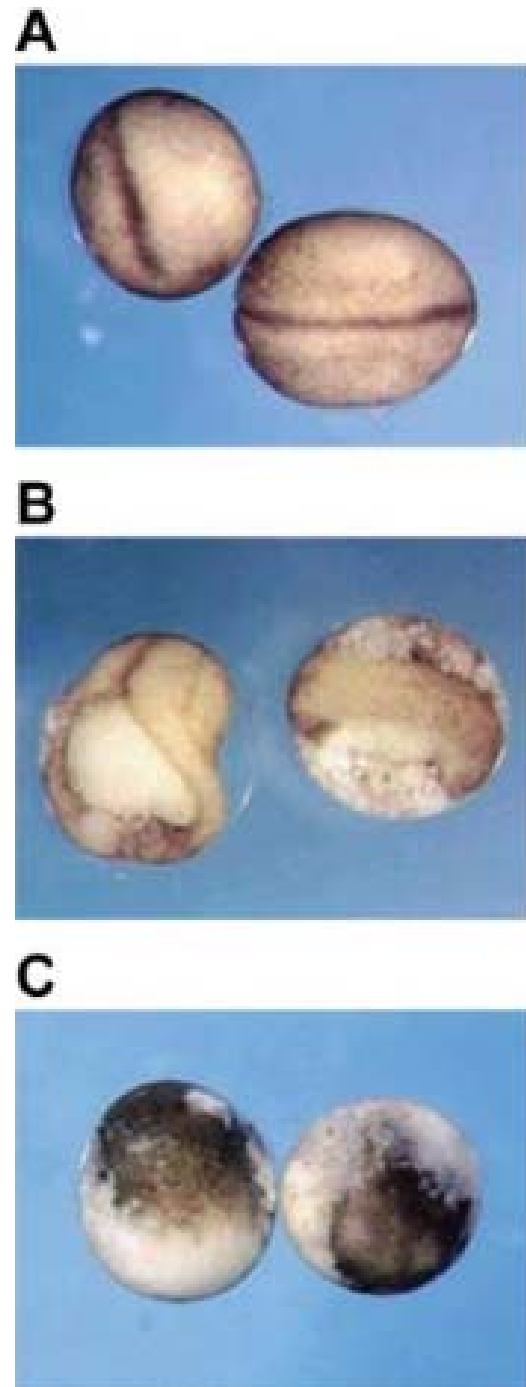


**FIGURE 4.** Deletion of endogenous *X-OAT* produces gastrulation defect and death of embryo. Either 5 ng or 10 ng of *X-OAT-Mo* was injected into the animal pole area of two-cell stage embryos. Embryos were cultured in 30% MMR solution and photographed at the equivalent of stage 13: (A) normal control; (B) injected with 5 ng *X-OAT-Mo*; (C) injected with 10 ng *X-OAT-Mo* photographed at stage 10.

molecular markers was performed by RT-PCR on RNA extracted from explants of embryos. At the two-cell stage, 1 ng of mRNAs encoding *X-OAT* sense or 5 ng *X-OAT-Mo* was injected into each of the two blastomeres of *Xenopus* embryos. The ACs were dissected at stages 8.5 to 9.0 and cultured until the equivalent of stage 22. The results in *X-OAT*-expressing ACs showed that the pan-neural marker NCAM<sup>43</sup> was decreased (Fig. 7A). In addition, anterior neural

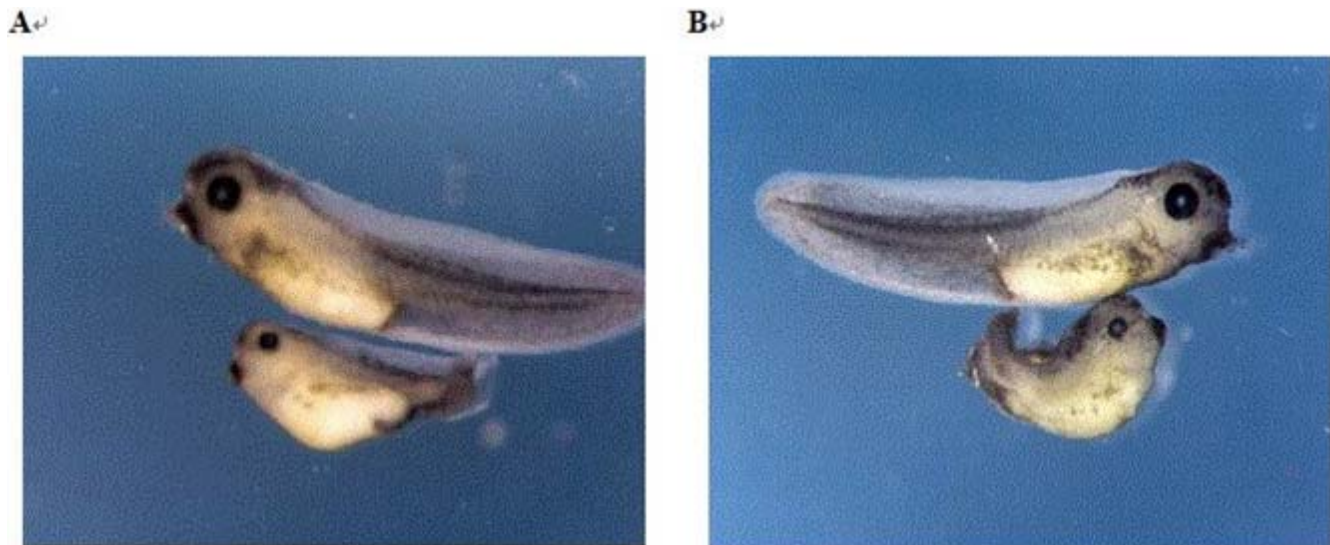


**FIGURE 5.** Overexpression of *X-OAT*-induced morphological change of *Xenopus* embryo. (A) *Top*: mRNA encoding  $\beta$ -gal (1 ng) served as negative control; *bottom*: *X-OAT* sense RNA (1 ng) was injected into animal pole area at the two-cell stage. (B) *Top*: mRNA encoding  $\beta$ -gal (1 ng) served as negative control; *bottom*: *X-OAT* sense RNA (1 ng) was injected into dorsal marginal zone of four-cell stage embryos.

marker *Otx2*<sup>44,45</sup> and posterior neural marker *HoxB9*<sup>46</sup> were also decreased or absent (Fig. 7B). These results were consistent with the phenotypic changes of ACs observed in Figure 6.

#### Analysis of Functional Activity of the *X-OAT* Mutants

We artificially generated four mutants, *X-OATR180T*, *X-OATR180T/L402P*, *X-OATL402P*, and *X-OATK292N*, because these mutations in humans result in GA (Fig. 8A). The mutants were confirmed by DNA sequencing. Messenger RNA was synthesized from wild-type (WT) and from each of the mutants. The mutants were translated at an efficiency similar to that for the WT *X-OAT* (Fig. 8B), suggesting that these mutations did not affect translatability. Thus, we used these mRNAs for the biological studies described below. To investigate the functional activity of the *X-OAT* during *Xenopus* embryonic development, we injected each of the mutants into the animal pole of the two-cell stage embryos. The injected embryos were allowed to develop until the tadpole stages, and the dorsoanterior index (DAI) was scored.<sup>47</sup> As shown in Table 1, the embryos injected with *X-OATWT*, *X-OATR180T*, *X-OATL402P*, or *X-OATK292N* mRNA were malformed with DAI of 2.5 (68%, simple sizes: 34/50), 2.3 (74%, simple sizes: 37/50), 2.8 (62% simple sizes: 31/50), and 2.6 (72%, simple sizes: 36/50), respectively. In contrast, the *X-OATR180T/L402P* mRNA-injected embryos, like the  $\beta$ -gal-injected control embryos, remained normal with DAI 5.0 for both (Fig. 9A). We also analyzed the neuralization-inhibiting activity of the *X-OAT* mutants in ACs. As shown in Figure 9B, the *X-OATWT*, *X-OATR180T* (M1), *X-OATL402P* (M3), and *X-OATK292N* (M4) mRNA-injected ACs developed an epidermal-like phenotype: basically round without a clear white/black delineation. On the other hand, the *X-OATR180T/L402P* (M2) mRNA-injected ACs, like the  $\beta$ -gal-injected control ACs, developed a neural-like phenotype: slightly swollen with one side white and the other side black (cement gland) (Fig. 9B). To confirm these results, we examined the expression of the pan-neural marker NCAM using RT-PCR assay. The NCAM was expressed only in the ACs injected with mRNA containing both R180T and L402P mutations (Fig. 9C). These results suggest that the double mutation was crucial for mitigating the neuralization inhibitory activity of *X-OAT*.

#### Enzyme Activity of OAT

We sought insight into the mechanism of *X-OAT* as a neuralization inhibitor by correlating this inhibitory activity with the catalytic activity of the protein encoded by the various mutant *X-OATs* harvested from the ACs. We used a specific radioisotopic assay and performed the assays in triplicate. Because there was considerable dilution of the injected *X-OAT* mRNA by stage 22, the level of enzyme activity measured in the ACs injected with *X-OATWT* was only 44% higher than that in the ACs injected with  $\beta$ -gal (125.3  $\pm$  2.0 and 86.6  $\pm$  22.0 pmol/h-mg, respectively). Nevertheless, it was readily apparent that the ACs injected with *X-OATR180T/L402P* were similar to those in the ACs injected with  $\beta$ -gal. By contrast, the ACs injected with *X-OATR180T*, *X-OATL402P*, and *X-OATK292N* had enzyme activities only slightly lower than that of ACs injected with *X-OATWT*, but ACs injected with *X-OAT-Mo* had lower than that ACs injected with  $\beta$ -gal (Fig. 10; Table 2). The pattern showed that the enzyme activities in the ACs correlated with the ability to inhibit the neuralization phenotype and endogenous enzyme activities are necessary for normal embryo development.

#### DISCUSSION

The *Xenopus* embryo developmental model provided an opportunity to evaluate the biological function of OAT in this context. *Xenopus* OAT was found to be highly homologous to OAT of human, mouse, rat, *C. elegans*, and *Drosophila*. Among these species, OAT was highly conserved at the amino acid level. The *X-OAT* is expressed in almost all *Xenopus* adult tissues and at every stage of early embryonic development. In situ hybridization studies showed that *X-OAT* expression was especially prominent in the neural cord at the tailbud stage (Fig. 3C). In loss-of-function studies, embryonic development arrested at the gastrulation stage, suggesting that maternal OAT is essential for *Xenopus* embryonic development. In gain-of-function studies, overexpression of *X-OAT* ventralized *Xenopus* embryos. To corroborate these morphologic findings, we examined neural development induced by retinoic acid and activin in the early stages of embryonic development by analyzing relevant molecular markers in explants. The pan-

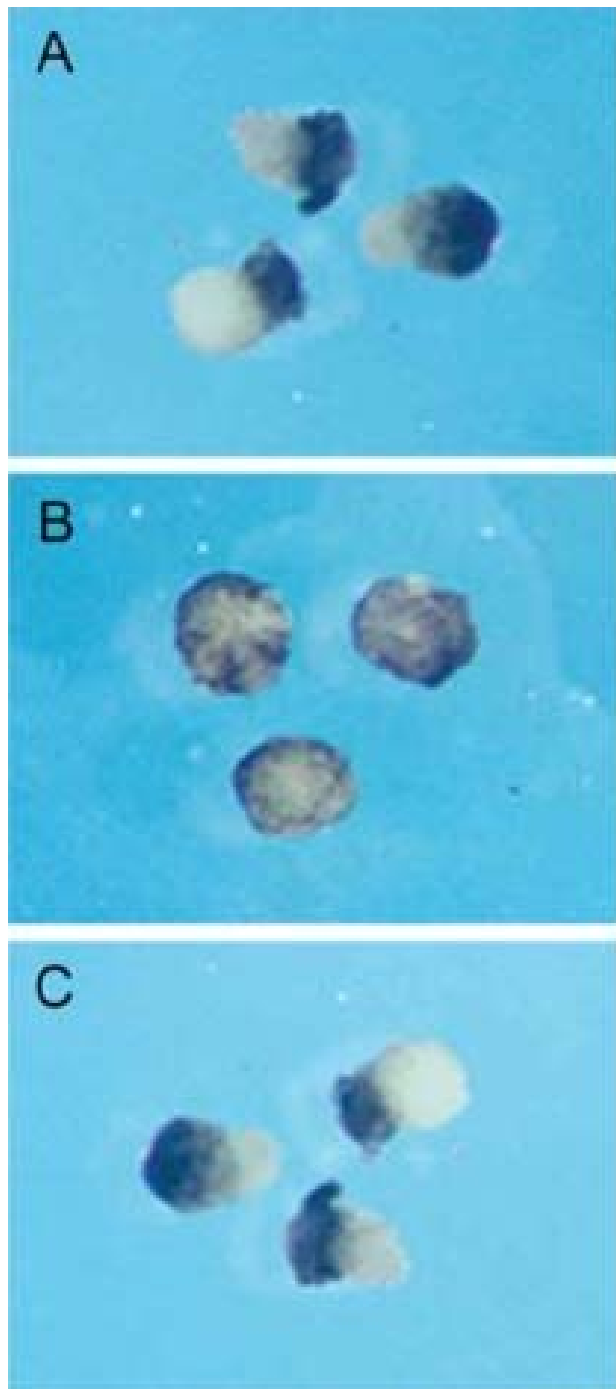


**FIGURE 6.** The OAT inhibited neuralization induced by activin and retinoic acid in *Xenopus* ACs. Two-cell stage embryos were injected in the animal pole area with mRNA (1 ng) encoding (A)  $\beta$ -gal, (B) sense X-OAT, or (C) X-OAT-Mo. The ACs were dissected at stages 8.5 to 9.0 and cultured in 67% Leibovitz's L-15 medium with activin (10 ng/mL) and retinoic acid ( $10^{-5}$  M) until they reached the equivalent of stage 22; three ACs of each group for photography. (A) All eight ACs appear slightly swollen with one side white and the other black (100%); (B) seven ACs appear mostly round and evenly brownish (88%), one AC has died; (C) the phenotype of all eight ACs similar to the (A) group's phenotype (100%).

neural marker NCAM, the anterior neural marker Otx2, and the posterior neural marker HoxB9 were all markedly decreased by exogenous X-OAT expression. These results are consistent with the ventralizing phenotype and suggest that OAT inhibits

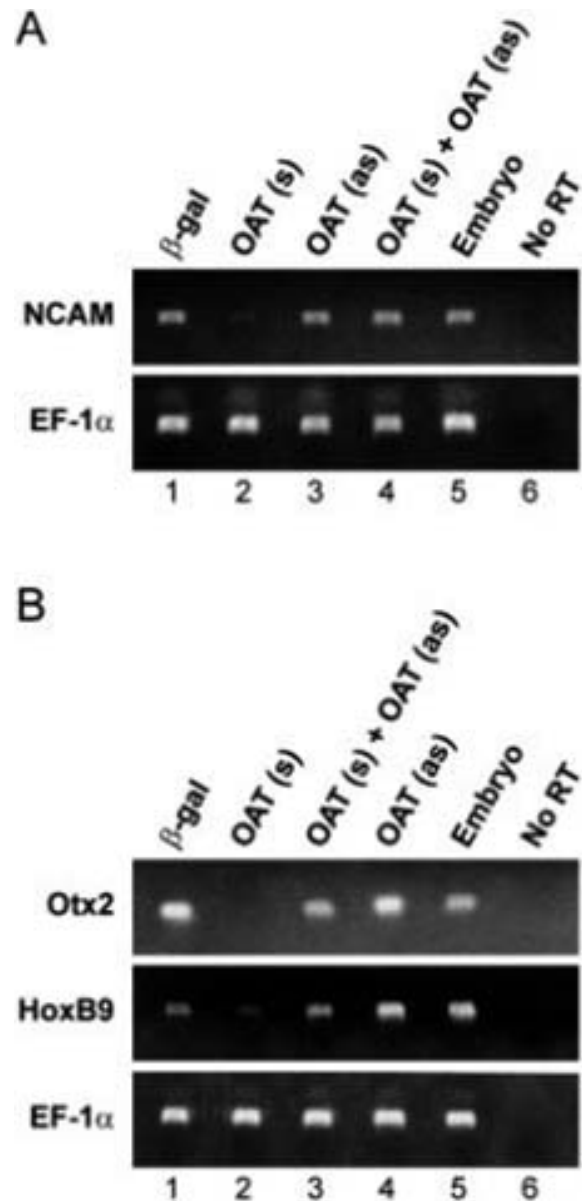


**FIGURE 7.** Inhibition of NCAM, HoxB9, and Otx2 expression by X-OAT in ACs cultured with activin and retinoic acid. The animal pole area of two-cell stage embryos was injected with mRNA encoding  $\beta$ -gal (1 ng), X-OAT, sense (s) (1 ng); X-OAT, sense (s) (1 ng) + X-OAT-Mo (as) (5 ng). The ACs were dissected at stages 8.5 to 9.0 and cultured in 67% Leibovitz's L-15 medium containing activin (10 ng/mL) and retinoic acid ( $10^{-5}$  M) until equivalent of stage 22. Total RNA was isolated from the ACs and assayed for expression by RT-PCR (A) for expression of NCAM, and (B) for expression of Otx2 and HoxB9. Expression of EF-1 $\alpha$  was used as loading control. Total RNAs from a whole embryo at the equivalent stage were used as a positive control. Controls with "No RT" reactions were performed with total RNAs obtained from the embryo and processed through the reactions without RT to confirm the absence of contaminating genomic DNA.

neurogenesis in ectodermal explants induced by retinoic acid and activin. It is of considerable interest that X-OAT may be involved in neural development. Although humans without OAT activity have no apparent developmental abnormality, they develop GA, which is associated with degeneration of the neuroretina and visual defects. In these individuals, neuromuscular and central nervous system abnormalities also have been described.<sup>48,49</sup> Thus, the abnormalities in *Xenopus* embryonic

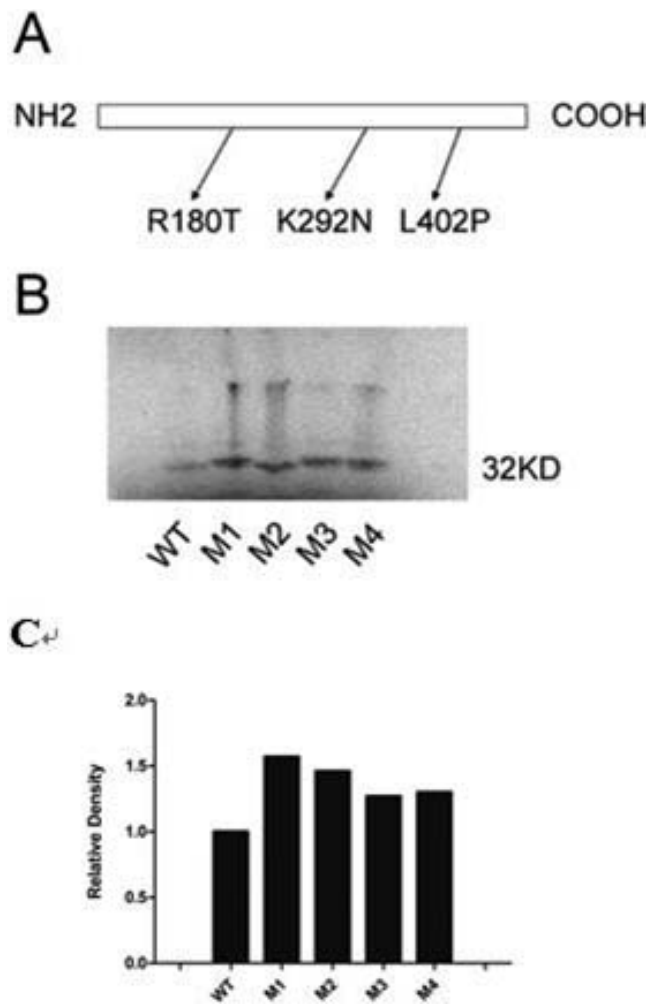


**FIGURE 8.** Translation of WT and mutated X-OATs. The introduced mutations are shown with their designations (A). The M2 has both the M1 and M3 mutations. M1: X-OATR180T; M2: X-OATR180T/L402P; M3: X-OATL402P; M4: X-OATK292N; WT: X-OATWT. Synthetic WT and mutated X-OAT mRNA were translated in a TNT-coupled reticulocyte lysate system (Promega) with [<sup>35</sup>S] methionine. Products were analyzed by autoradiography on an SDS Tris-HCl gel. A 32-kDa band appeared at similar intensity in all the lanes loaded with the translation products (B) and the densitometric analysis (C).

**TABLE 1.** Comparison of Dorsalizing Activity of X-OAT and Its Mutants

mRNA Injected	DAI Score	%
X-OATWT	2.5	68 (n: 34/50, d: 8/50)
X-OATR180T	2.3	74 (n: 37/50, d: 5/50)
X-OAT R180T/L402P	5.0	92 (n: 46/50, d: 4/50)
X-OATL402P	2.8	62 (n: 31/50, d: 9/50)
X-OATK292N	2.6	72 (n: 36/50, d: 7/50)
β-gal	5.0	96 (n: 48/50, d: 2/50)

Note: 1 ng mRNA encoding X-OAT or each of the X-OAT mutants was injected into the animal pole at two-cell stage embryos. The embryos were allowed to develop to tailbud stage and were scored for DAI. A normal embryo was scored 5, a completely ventralized embryo was scored 0, and a completely dorsalized embryo was scored 10. Other intermediate phenotypes were scored between 0 and 10, according to their degree of ventralization or dorsalization. n, the number of embryos; d, embryos that died.

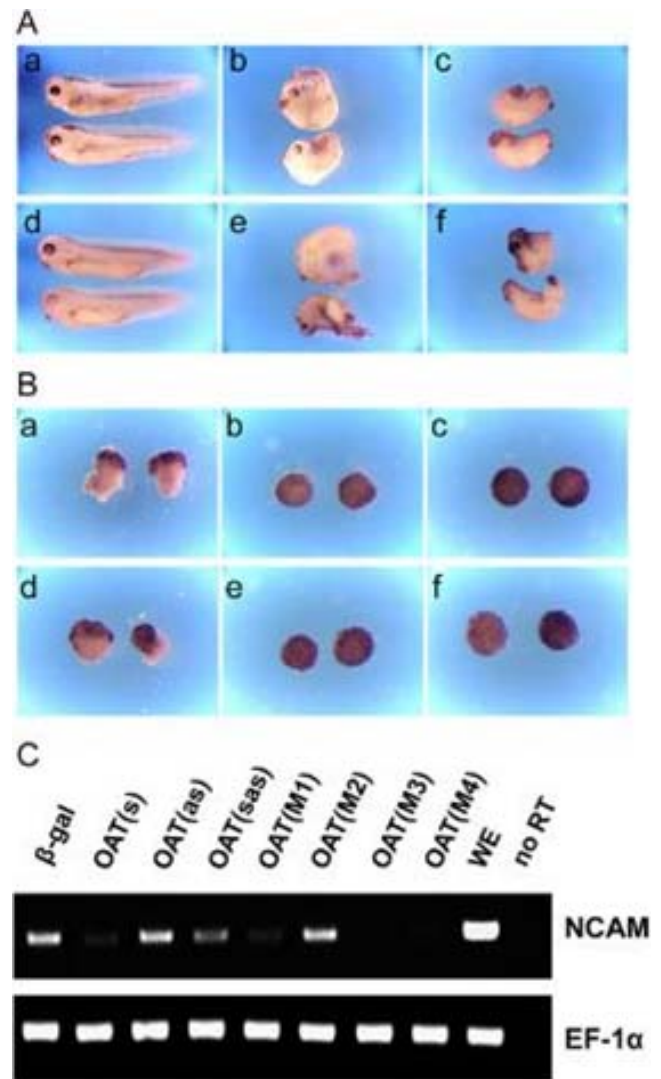


**FIGURE 9.** Phenotype observations and RT-PCR analysis of ACs expressing WT and mutated X-OAT; β-gal or 1 ng mRNA encoding WT or each of the X-OAT mutants was injected into the animal pole at the two-cell stage. (A) Embryos were grown to tadpole stage for photography. (a) β-gal (normal: 48/50, died: 2/50), (b) X-OATWT (normal: 8/50, ventralization: 34/50, died: 8/50), (c) X-OATR180T (M1) (normal: 8/50, ventralization: 37/50, died: 5/50), (d) X-OATR 180T/L402P (M2) (normal: 46/50, died: 4/50), (e) X-OATL402P (M3) (normal: 10/50, ventralization: 31/50, died: 9/50), or (f) X-OATK292N (M4) (normal: 7/50, ventralization: 36/50, died: 7/50). (B) The ACs were dissected at stage 8.5 to 9.0 and cultured to equivalent of stage 22. The ACs were harvested for photography: (a) β-gal (neuroization 8/8), (b) X-OATWT (normal: 8/8), (c) X-OATR180T (M1) (normal: 8/8), (d) X-OATR 180T/L402P (M2) (neuroization: 7/8, died: 1/8), (e) X-OATL402P (M3) (normal: 8/8) or (f) X-OATK292N (M4) (normal: 7/8, died: 1/8), or (C) for RT-PCR analysis of NCAM expression with EF-1α as control.

development with either loss- or gain-of-function in OAT may represent a more severe expression not found in mammalian species with overlapping metabolic pathways. There are examples of genes and their homologues, respectively, implicated in late-onset human disease, which play a critical developmental role in lower organisms.<sup>29,30</sup> Although the genetic or metabolic mechanisms of OAT on development remain unknown, the findings of OAT on *Xenopus* embryonic development may serve as a model for the neurological changes in GA. The more than 60 OAT mutations resulting in

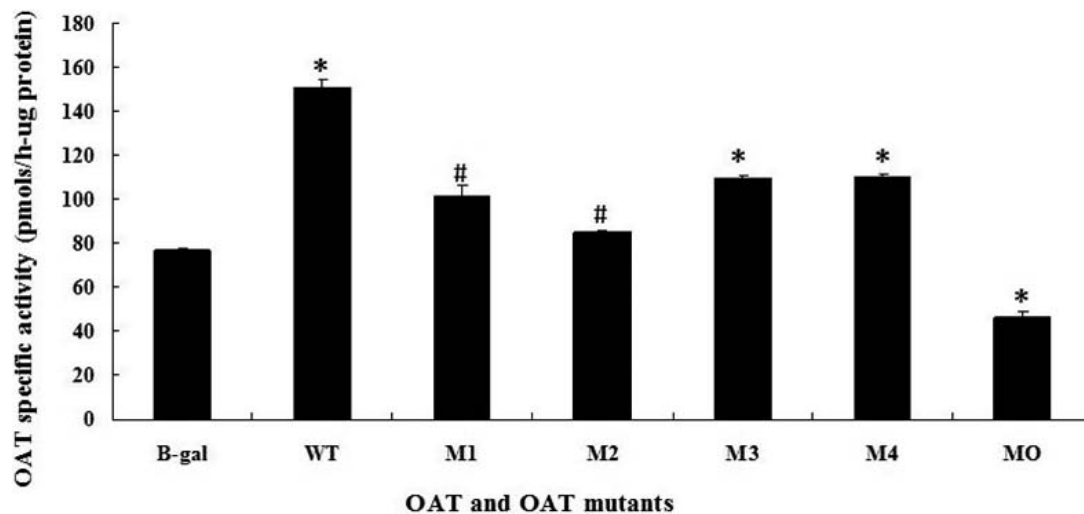


**FIGURE 10.** Differential X-OAT enzyme activities in ACs expressing  $\beta$ -gal, X-OAT-Mo, X-OATWT, and mutants. Messenger RNA (1 ng) from X-OATWT or mutants was injected into the animal pole at the two-cell stage. The ACs were dissected at stage 8.5 to 9.0 and cultured to equivalent of stage 22. The ACs were harvested in PBS buffer (16 ACs per group) for protein concentration measurement and X-OAT enzyme activity assay (see Methods). All groups were assayed in triplicate. *P* values are compared between  $\beta$ -gal and each OAT by Student's *t*-tests. \**P* < 0.01, compared with  $\beta$ -gal; \*\**P* < 0.001, compared with  $\beta$ -gal.

GA in humans provided a starting point for our analysis of the functional relationship of X-OAT in the *Xenopus* embryonic model.<sup>17,33,35</sup> We constructed X-OAT mutations analogous to the mutations in humans that cause the GA phenotype and loss of catalytic activity. However, in comparison with X-OATWT, single mutations resulting in X-OATR180T, X-OATL402P, and X-OATK292N did not mitigate the inhibition of neuralization activity (i.e., they inhibited neuralization the same as WT). However, when both R180T and L402P mutations were present in X-OATR180T/L402P, the inhibitory effect on neuralization was abrogated (Figs. 9A-C; Table 1). Of the aforementioned mutations used, all were situated in the conserved region of the OAT gene<sup>12</sup>; in cells from GA patients, these mutated genes yielded normal amounts and size of OAT mRNA. The R180T and L402P mutant alleles from Finnish patients with GA were described by Mitchell et al.<sup>35</sup> In studies of OAT from these patients, these investigators found that L402P apparently destabilizes the structure of the enzyme, leading to degradation and decreased amounts of immunoreactive protein. On the other hand, R180T results in an inactive enzyme without reducing the amount of OAT antigen.<sup>11,33</sup>

Because of the divergence between humans and *Xenopus* in the phenotypic consequence of these mutations, it was important to characterize the effect of these mutations on

enzyme activity in *Xenopus*. Using a specific radioisotopic assay, we determined OAT activity in extracts from ACs (stage 22) injected with various X-OAT mRNAs at the two-cell stage. As shown in Figure 9, embryos injected with X-OATWT increased their OAT activity approximately 45% over controls injected with  $\beta$ -gal. The dilutional loss of mRNA up to stage 22 probably limited the increase to this modest level, and it is likely that the relative contribution of exogenous X-OAT was considerably greater at earlier stages. Strikingly, the effect of the mutations on enzyme activity, or rather the lack of effect of certain mutations, paralleled the failure of these mutations to mitigate the profound alterations in developmental phenotype. X-OATR180T, X-OATL402P, and X-OATK292N had little effect on enzyme activity. However, the double mutant X-OATR180T/L402P appeared to have completely lost enzyme activity and was no different from control explants injected with  $\beta$ -gal. In the study by Brody et al.<sup>17</sup> using GA fibroblasts, and also in the study using lymphocytes from Finnish GA patients,<sup>33</sup> OAT mutants R180T and R154L have no measurable enzyme function but have OAT antigen. In humans, the loss of activity due to these point mutations is likely due to loss of protein conformation and stability.<sup>50,51</sup> It may be that this loss of conformation is temperature-sensitive (i.e., loss of conformation and activity occurs at 37°C for human OAT but not for either embryonic development at 14–18°C or embryonic activity at 24°C). The double mutation, on the other hand, which resulted in loss of both measured enzyme activity and the ability to modulate phenotype, most likely yielded a protein without active conformation at the relevant temperatures. This explanation, however, does not account for the retention of activity in X-OATK292N because lysine 292 is the binding site for pyridoxal phosphate. We will undertake additional studies to distinguish these physical and catalytic properties of mutant OAT at various temperatures.

Nevertheless, the enzymatic activity residing in the various X-OAT mutants followed the same pattern as their ability to ventralize and inhibit neuralization (Figs. 9A-C) and suggests that the modulation of the developmental phenotype resides in the metabolic activity of X-OAT. This enzyme catalyzes reactions at the central juncture in the pathways of amino acid intermediary metabolism<sup>11</sup> and produces glutamic- $\gamma$ -semi-aldehyde, which is in tautomeric equilibrium with P5C. The

**TABLE 2.** Enzyme Activities of X-OAT in ACs Expressed  $\beta$ -gal, X-OAT, and X-OAT Mutants

Gene Expression	Net DPM	X-OAT Activity, pmol/h-ug Protein
$\beta$ -gal	2933.24 $\pm$ 54.67	76.42 $\pm$ 0.88
X-OAT WT	5255.68 $\pm$ 116.79*	150.66 $\pm$ 3.64*
X-OAT M1	4062.04 $\pm$ 57.14*	101.7 $\pm$ 4.79†
X-OAT M2	3574.64 $\pm$ 46.13*	84.68 $\pm$ 1.14†
X-OAT M3	5808.28 $\pm$ 85.09*	109.58 $\pm$ 1.42*
X-OAT M4	6577.63 $\pm$ 35.20*	110.58 $\pm$ 0.89*
X-OAT-Mo	2741.41 $\pm$ 151.57	46.16 $\pm$ 2.43*

Data are mean  $\pm$  SD. The assays were performed in triplicate. *P* values are compared between  $\beta$ -gal and each OAT by Student's *t*-tests.

\* *P* < 0.001, compared with  $\beta$ -gal.

† *P* < 0.01, compared with  $\beta$ -gal.

latter can profoundly affect certain metabolic pathways.<sup>2</sup> Recent studies have shown that the metabolic cycling of proline and P5C by proline oxidase and P5C reductase, respectively, may play important roles in several disease processes. The expression of proline oxidase responds to p53,<sup>52</sup> PPAR $\gamma$ -activating ligands,<sup>53</sup> and rapamycin,<sup>54</sup> representing respective signaling due to genotoxic, inflammatory, and nutrient stress.<sup>55,56</sup> Doimo et al.<sup>57</sup> found that 5-aminoimidazole-4-carboxamide ribonucleoside markedly stimulates OAT expression, thus representing a possible treatment for a subset of GA patients with hypomorphic alleles. Overexpression of proline oxidase (POX) results not only in cell cycle blockade and apoptosis,<sup>58</sup> but also produces ATP for cell maintenance.<sup>53</sup> Mutations resulting in loss of POX activity increase the risk for schizophrenia,<sup>7,59</sup> and the disappearance of POX during tumorigenesis suggests that it functions as a cancer-suppressor protein.<sup>58</sup> Just how these demonstrated mechanisms in carcinogenesis relate to the observed developmental abnormalities remain unclear. The absence of OAT in humans does not have a clinical phenotype until later in life. We supposed this is because the genes of the proline-arginine-glutamate pathway are epistatic. Neurodevelopmental abnormalities are associated with mutations in P5C synthase, which converts glutamate to P5C.<sup>9,10</sup> Investigators have recently reported that neurological abnormalities are also associated with mutations in P5C reductase, which converts P5C back to proline, and morpholino knockdown of PYCR1 in both *Xenopus* and zebrafish, cause developmental defects.<sup>60</sup> These more recent findings further support the importance of this pathway in neurodevelopment. Whatever the mechanism, our findings provide robust, direct evidence that perturbations of P5C synthesis by OAT is associated with striking abnormalities in neurodevelopment. Furthermore, in mammalian development, the production of ornithine and arginine from proline and P5C is mediated by OAT.<sup>61,62</sup> Arginine is not only an important amino acid for protein synthesis, but also is the precursor for nitric oxide, an important neurotransmitter and regulatory molecule.<sup>63</sup> Ornithine, the substrate for OAT, is also the substrate for ornithine decarboxylase, which catalyzes the formation of putrescine, a critical intermediate in the synthesis of polyamines, a family of compounds known to play important roles in proliferation and differentiation.<sup>64,65</sup> Although the linkage of metabolic activity and phenotypic modulation provides an attractive hypothesis, it may be that the phenotypic changes observed in our studies are a novel function independent of enzymatic activity. For example, the ventralized phenotype of *Xenopus* embryos induced by OAT overexpression is very similar to the phenotype produced by activated BMP-4 and inhibited Wnt signaling. This may provide a clue that OAT is linked to growth factor or the Wnt pathway-mediated neurogenesis. Conversely, OAT overexpression may activate or interfere with as-yet-undefined pathways during embryonic development. Recent demonstration that metabolic enzymes may play a role in gene switching may serve as a model.<sup>66</sup> Our data presented here suggest that maternal X-OAT is essential for *Xenopus* embryonic development, but overexpression of X-OAT suppresses neuralization activity. It is possible that X-OAT plays a critical role in the regulation of early embryogenesis, especially in neurogenesis.

### Acknowledgments

We thank David Valle, MD, Johns Hopkins University School of Medicine, for his helpful comments.

Supported in part by a grant from National Natural Science Foundation of China (NSFC) (305705890, 31070953) from China (YP); the International Collaboration Program of Universities in Guangdong Province (2012gjh001 to YP); and the Intramural

Research Program of the NIH, National Cancer Institute, Center for Cancer Research and has been funded in part with Federal funds from the National Cancer Institute, NIH under contract no. HHSN27612080001. The authors alone are responsible for the content and writing of the paper.

Disclosure: **Y. Peng**, None; **S.K. Cooper**, None; **Y. Li**, None; **J.M. Mei**, None; **S. Qiu**, None; **G.L. Borchert**, None; **S.P. Donald**, None; **H.-F. Kung**, None; **J.M. Phang**, None

### References

- Hagedorn CH, Phang JM. Catalytic transfer of hydride ions from NADPH to oxygen by the interconversions of proline and delta 1-pyrroline-5-carboxylate. *Arch Biochem Biophys*. 1986; 248:166-174.
- Phang JM. The regulatory functions of proline and pyrroline-5-carboxylic acid. *Curr Top Cell Regul*. 1985;25:91-132.
- Fremeau RT Jr, Caron MG, Blakely RD. Molecular cloning and expression of a high affinity L-proline transporter expressed in putative glutamatergic pathways of rat brain. *Neuron*. 1992;8: 915-926.
- Renick SE, Kleven DT, Chan J, et al. The mammalian brain high-affinity L-proline transporter is enriched preferentially in synaptic vesicles in a subpopulation of excitatory nerve terminals in rat forebrain. *J Neurosci*. 1999;19:21-33.
- Gogos JA, Santha M, Takacs Z, et al. The gene encoding proline dehydrogenase modulates sensorimotor gating in mice. *Nat Genet*. 1999;21:434-439.
- Liu H, Heath SC, Sobin C, et al. Genetic variation at the 22q11 PRODH2/DGCR6 locus presents an unusual pattern and increases susceptibility to schizophrenia. *Proc Natl Acad Sci U S A*. 2002;99:3717-3722.
- Bender HU, Almashanu S, Steel G, et al. Functional consequences of PRODH missense mutations. *Am J Hum Genet*. 2005;76:409-420.
- Phang JM, Hu CA, Valle D. Disorders of proline and hydroxyproline metabolism. In: *The Metabolic and Molecular Bases of Inherited Disease*. 8th ed. New York: McGraw-Hill; 2001:1821-1838.
- Baumgartner MR, Hu CA, Almashanu S, et al. Hyperammonemia with reduced ornithine, citrulline, arginine and proline: a new inborn error caused by a mutation in the gene encoding delta(1)-pyrroline-5-carboxylate synthase. *Hum Mol Genet*. 2000;9:2853-2858.
- Bicknell LS, Pitt J, Aftimos S, Ramadas R, Maw MA, Robertson SP. A missense mutation in ALDH18A1, encoding Delta1-pyrroline-5-carboxylate synthase (P5CS), causes an autosomal recessive neurocutaneous syndrome. *Eur J Hum Genet*. 2008; 16:1176-1186.
- Valle D, Simell O. The hyperornithinemias. In: *The Metabolic and Molecular Bases of Inherited Disease*. 8th ed. New York: McGraw-Hill Press; 2001:1857-1895.
- Valle D, Simell O. The hyperornithinemias. In: *The Metabolic and Molecular Bases of Inherited Disease*. 7th ed. New York: McGraw-Hill Press; 1995:1147-1185.
- Kaiser-Kupfer MI, Ludwig IH, de Monasterio FM, Valle D, Krieger I. Gyrate atrophy of the choroid and retina. Early findings. *Ophthalmology*. 1985;92:394-401.
- Takki KK, Milton RC. The natural history of gyrate atrophy of the choroid and retina. *Ophthalmology*. 1981;88:292-301.
- Simell O, Takki K. Raised plasma-ornithine and gyrate atrophy of the choroid and retina. *Lancet*. 1973;1:1031-1033.
- Valle D, Kaiser-Kupfer MI, Del Valle LA. Gyrate atrophy of the choroid and retina: deficiency of ornithine aminotransferase in transformed lymphocytes. *Proc Natl Acad Sci U S A*. 1977;74: 5159-5161.

17. Brody LC, Mitchell GA, Obie C, et al. Ornithine delta-aminotransferase mutations in gyrate atrophy. Allelic heterogeneity and functional consequences. *J Biol Chem.* 1992;267:3302-3307.
18. Inana G, Totsuka S, Redmond M, et al. Molecular cloning of human ornithine aminotransferase mRNA. *Proc Natl Acad Sci U S A.* 1986;83:1203-1207.
19. Michaud J, Brody LC, Steel G, et al. Strand-separating conformational polymorphism analysis: efficacy of detection of point mutations in the human ornithine delta-aminotransferase gene. *Genomics.* 1992;13:389-394.
20. Mitchell GA, Looney JE, Brody LC, et al. Human ornithine-delta-aminotransferase. cDNA cloning and analysis of the structural gene. *J Biol Chem.* 1988;263:14288-14295.
21. Ramesh V, Shaffer MM, Allaire JM, Shih VE, Gusella JF. Investigation of gyrate atrophy using a cDNA clone for human ornithine aminotransferase. *DNA.* 1986;5:493-501.
22. Wang T, Lawler AM, Steel G, Sipila I, Milam AH, Valle D. Mice lacking ornithine-delta-aminotransferase have paradoxical neonatal hypoorithinaemia and retinal degeneration. *Nat Genet.* 1995;11:185-190.
23. Bisailon JJ, Radden LA II, Szabo, ET, et al. The retarded hair growth (rhg) mutation in mice is an allele of ornithine aminotransferase (OAT). *Mol Genet Metab Rep.* 2014;1:378-390.
24. Wang T, Steel G, Milam AH, Valle D. Correction of ornithine accumulation prevents retinal degeneration in a mouse model of gyrate atrophy of the choroid and retina. *Proc Natl Acad Sci U S A.* 2000;9:1224-1229.
25. Tseng HT, Shah R, Jamrich M. Function and regulation of FoxF1 during *Xenopus* gut development. *Development.* 2004;131:3637-3647.
26. Nitta KR, Tanegashima K, Takahashi S, Asashima M. XSIP1 is essential for early neural gene expression and neural differentiation by suppression of BMP signaling. *Dev Biol.* 2004;275:258-267.
27. Newport J, Kirschner M. A major developmental transition in early *Xenopus* embryos: II. Control of the onset of transcription. *Cell.* 1982;30:687-696.
28. Sullivan SA, Akers L, Moody SA. FoxD5a, a *Xenopus* winged helix gene, maintains an immature neural ectoderm via transcriptional repression that is dependent on the C-terminal domain. *Dev Biol.* 2001;232:439-457.
29. Hong CS, Koo EH. Isolation and characterization of *Drosophila* presenilin homolog. *Neuroreport.* 1997;8:665-668.
30. Jarriault S, Greenwald I. Suppressors of the egg-laying defective phenotype of sel-12 presenilin mutants implicate the CoREST corepressor complex in LIN-12/Notch signaling in *C. elegans*. *Genes Dev.* 2002;16:2713-2728.
31. Sive HL, Grainger RM, Harland RM. Early development of *Xenopus laevis*. In: *A Laboratory Manual*. New York: Cold Spring Harbor Laboratory Press; 2000:1-35.
32. De Jonge WJ, Dingemans MA, de Boer PA, Lamers WH, Moorman AF. Arginine-metabolizing enzymes in the developing rat small intestine. *Pediatr Res.* 1998;43:442-451.
33. Heinanen K, Nanto-Salonen K, Leino L, et al. Gyrate atrophy of the choroid and retina: lymphocyte ornithine-delta-aminotransferase activity in different mutations and carriers. *Pediatr Res.* 1998;44:381-385.
34. Inana G, Chambers C, Hotta Y, et al. Point mutation affecting processing of the ornithine aminotransferase precursor protein in gyrate atrophy. *J Biol Chem.* 1989;264:17432-17436.
35. Mitchell GA, Brody LC, Sipila I, et al. At least two mutant alleles of ornithine delta-aminotransferase cause gyrate atrophy of the choroid and retina in Finns. *Proc Natl Acad Sci U S A.* 1989;86:197-201.
36. Peng Y, Xu RH, Mei JM, et al. Neural inhibition by c-Jun as a synergizing factor in bone morphogenetic protein 4 signaling. *Neuroscience.* 2002;109:657-664.
37. Phang JM, Downing SJ, Valle DL, Kowaloff EM. A radioisotopic assay for proline oxidase activity. *J Lab Clin Med.* 1975;85:312-317.
38. Fukui A, Nakamura T, Uchiyama H, Sugino K, Sugino H, Asashima M. Identification of activins A, AB, and B and follistatin proteins in *Xenopus* embryos. *Dev Biol.* 1994;163:279-281.
39. Durston AJ, Timmermans JP, Hage WJ, et al. Retinoic acid causes an anteroposterior transformation in the developing central nervous system. *Nature.* 1989;340:140-144.
40. Uochi T, Asashima M. XCIRP (*Xenopus* homolog of cold-inducible RNA-binding protein) is expressed transiently in developing pronephros and neural tissue. *Gene.* 1998;211:245-250.
41. Cheung WK, Yang PH, Huang QH, et al. Identification of protein domains required for makorin-2-mediated neurogenesis inhibition in *Xenopus* embryos. *Biochem Biophys Res Commun.* 2010;394:18-23.
42. Yang PH, Cheung WK, Peng Y, et al. Makorin-2 is a neurogenesis inhibitor downstream of phosphatidylinositol 3-kinase/Akt (PI3K/Akt) signal. *J Biol Chem.* 2008;283:8486-8495.
43. Kintner CR, Melton DA. Expression of *Xenopus* N-CAM RNA in ectoderm is an early response to neural induction. *Development.* 1987;99:311-325.
44. Blitz IL, Cho KW. Anterior neurectoderm is progressively induced during gastrulation: the role of the *Xenopus* homeobox gene orthodenticle. *Development.* 1995;121:993-1004.
45. Pannese M, Polo C, Andreazzoli M, et al. The *Xenopus* homologue of Otx2 is a maternal homeobox gene that demarcates and specifies anterior body regions. *Development.* 1995;121:707-720.
46. Wright CV, Morita EA, Wilkin DJ, De Robertis EM. The *Xenopus* XIHbox 6 homeo protein, a marker of posterior neural induction, is expressed in proliferating neurons. *Development.* 1990;109:225-234.
47. Kao KR, Elinson RP. The entire mesodermal mantle behaves as Spemann's organizer in dorsoanterior enhanced *Xenopus laevis* embryos. *Dev Biol.* 1988;127:64-77.
48. Peltola KE, Nanto-Salonen K, Heinonen OJ, et al. Ophthalmologic heterogeneity in subjects with gyrate atrophy of choroid and retina harboring the L402P mutation of ornithine aminotransferase. *Ophthalmology.* 2001;108:721-729.
49. Valtonen M, Nanto-Salonen K, Jaaskelainen S, et al. Central nervous system involvement in gyrate atrophy of the choroid and retina with hyperornithinaemia. *J Inher Metab Dis.* 1999;22:855-866.
50. Kesavan P, Wang L, Davis E, et al. Structural instability of mutant beta-cell glucokinase: implications for the molecular pathogenesis of maturity-onset diabetes of the young (type-2). *Biochem J.* 1997;322:57-63.
51. Kanno H, Fujii H, Miwa S. Expression and enzymatic characterization of human glucose phosphate isomerase (GPI) variants accounting for GPI deficiency. *Blood Cells Mol Dis.* 1998;24:54-61.
52. Polyak K, Xia Y, Zweier JL, Kinzler KW, Vogelstein B. A model for p53-induced apoptosis. *Nature.* 1997;389:300-305.
53. Pandhare J, Cooper SK, Phang JM. Proline oxidase, a proapoptotic gene, is induced by troglitazone: evidence for both peroxisome proliferator-activated receptor gamma-de-

- pendent and -independent mechanisms. *J Biol Chem.* 2006; 281:2044–2052.
54. Pandhare J, Donald SP, Cooper SK, Phang JM. Regulation and function of proline oxidase under nutrient stress. *J Cell Biochem.* 2009;107:759–768.
55. Phang JM, Donald SP, Pandhare J, Liu Y. The metabolism of proline, a stress substrate, modulates carcinogenic pathways. *Amino Acids.* 2008;35:681–690.
56. Phang JM, Pandhare J, Zahirnyk O, Liu Y. PPARgamma and proline oxidase in cancer. *PPAR Res.* 2008;2008:542694.
57. Doimo M, Desbats MA, Baldoïn MC, et al. Functional analysis of missense mutations of OAT, causing gyrate atrophy of choroid and retina. *Hum Mutat.* 2013;34:229–236.
58. Liu Y, Borchert GL, Surazynski A, Phang JM. Proline oxidase, a p53-induced gene, targets COX-2/PGE2 signaling to induce apoptosis and inhibit tumor growth in colorectal cancers. *Oncogene.* 2008;27:6729–6737.
59. Willis A, Bender HU, Steel G, Valle D. PRODH variants and risk for schizophrenia. *Amino Acids.* 2008;35:673–679.
60. Reversade B, Escande-Beillard N, Dimopoulou A, et al. Mutations in PYCR1 cause cutis laxa with progeroid features. *Nat Genet.* 2009;41:1016–1021.
61. Hu CA, Lin WW, Obie C, Valle D. Molecular enzymology of mammalian Delta1-pyrroline-5-carboxylate synthase. Alternative splice donor utilization generates isoforms with different sensitivity to ornithine inhibition. *J Biol Chem.* 1999;274: 6754–6762.
62. Wu G. Synthesis of citrulline and arginine from proline in enterocytes of postnatal pigs. *Am J Physiol.* 1997;272:G1382–G1390.
63. Wu G, Morris SM Jr. Arginine metabolism: nitric oxide and beyond. *Biochem J.* 1998;336:1–17.
64. Luk GD, Casero RA Jr. Polyamines in normal and cancer cells. *Adv Enzyme Regul.* 1987;26:91–105.
65. Pegg AE. Polyamine metabolism and its importance in neoplastic growth and a target for chemotherapy. *Cancer Res.* 1988;48:759–774.
66. Zheng L, Roeder RG, Luo Y. S phase activation of the histone H2B promoter by OCA-S, a coactivator complex that contains GAPDH as a key component. *Cell.* 2003;114:255–266.